Eng. & Technology, Vol.25, No.4, 2007

The Effect of Size and Location of a Heating Source on the Buoyant Flow in a Heated Space

Asst. Prof. Waheed S. Mohammed* Asst. Lect.Gazy F. Saloomy*
Asst. Lect. Abdul-Jabar Muttair Ahmed**
Received on: 10/5/2005
Accepted on: 25/10/2005

Abstract

A numerical study of two-dimensional turbulent buoyant recirculating flows within a heated space is presented. The study involves the solution of elliptic partial differential equations for the conservation of mass, momentum, energy, turbulence energy and its dissipation rate. These equations were solved together with algebraic expressions for the turbulent viscosity and heat diffusivity in a finite difference form. The simulations of the turbulent buoyant flow within the space were undertaken using two principle geometrical arrangements (A & B) of the room with different locations and sizes of a heating source (b/h=0.08, 0.28, and 0.5 for geometry A and b/h=0.75, 1.45, and 6.0 for geometry B). The study demonstrates that for a thermal comfort conditions in the space the location and size of the heating source are of great importance. When the heating source is located in the middle of the floor it is found to generate a high velocity air stream resulted from vortices produce a local thermal discomfort in the occupation zone. On the other hand its location under a cold window offsets the losses in heat and avoiding the form of the high velocity air streams in the occupation zone. The size of the heating source is also found to influence the occupation zone condition through the effect on the heat transfer rate inside the conditioned space.

تأثير حجم وموقع المصدر الحراري على الجريان الطفوي في غرفة مسخنة

الخلاصة

تم عرض دراسة حاسوبية لجريانات دورانية مضطربة طفوية ثنائية البعد داخل حيز مسخن. تضمنت الدراسة حل المعادلات الجزئية الاهليلجية المتمثلة بحفظ الكتلة، الزخم، الطاقة و الطاقة المضطربة ومعدل ضياعها. لقد حلت هذه المعادلات سوية مع الصيغ الجبرية للزوجة المضطربة وانتشارية الحرارة باستخدام تقنية الفروقات المحددة. تم أجراء حسابات لجريان مضطرب طفوي داخل غرفة باستخدام ترتيبين هند سيين رئيسين للغرفة (A و B) مع وجود مصدر حراري بمواقع وأحجام مختلفة (b/h=٠,٠٨، ٠,٢٨، و ٠,٥ للترتيب A و b/h=٠,٧٥، ١,٤٥، و ٦,٠ للترتيب B). الدراسة قد وضحت ان لموقع وحجم المصدر الحراري تأثير مهم على الظروف الحرارية داخل الحيز. فعندما يكون موقع المصدر الحراري في منتصف الغرفة فانه يولد تيارات هواء ذات سرعة عالية نسبيا ناتجة عن دوامات تسببها حركة الهواء البارد الى اسفل وحركة الهواء الحار الى الأعلى. وتسبب هذه الدوامات ظروف حرارية غير ملائمة داخل الحيز المشغول. وعندما يكون موقعه اسفل الشباك البارد فانه يعادل الخسارة في الحرارة ويجنبنا تولد تيارات الهواء ذات السرعة العالية داخل الحيز المشغول. كذللك قد لوحظ أن لحجم المصدر الحراري تاثير على ظروف الحيز المشغول من خلال تاثيره على معدل انتقال الحرارة داخل الحيز المكيف.

* Mechanical Engineering Department, UOT.
** Technical Education Department, UOT.,

http s://doi.org/10.30684/etj.25.4.3
2412-0758/University of Technology-Iraq, Baghdad, Iraq

Definition	
a_E ,a_W , a_N , a_P a_S,	Coefficient of general Finite-Difference equation
B	The source term in general Finite-Difference equation.
b	Heating source length (m) .
C_1, C_2, C_d	Coefficients in turbulence model.
C_P	Specific heat transfer (J/kg.K).
D	Diffusion term.
F	Convection coefficient.
G_k	Generation rate of turbulence energy.
G_B	Buoyancy production.
g	Gravitational acceleration (m/s^2).
H, L	Room height & length (m).
h	Heating source height (m) .
h_{cx}	Local heat transfer coefficient ($W/m^2.K$).
k	Turbulent kinetic energy (m^2/s).
k_c	Thermal conductivity (W/m.K).
Nu	Local nusselt number.
n	Normal to the wall.
P	Static pressure (N/m^2).
Pe	Peclet number.
R_Φ	Residual source.
S_Φ	General source term.
$\Delta x, \Delta y$	Finite-Difference cell dimensions (m).
T	Time-average temperature (K).
T_m	Mean temperature (K).
T_W	Wall Temperature (K).
S_{vx}, $S_{vy,}$ S_T	Source term in V_x-momentum, V_y -momentum and energy equation
x, y	Cartesian coordinates.
Greek symbols	
β	Thermal expansion coefficient.
Φ	Time average general scalar Property.
ε	The dissipation rate of Turbulence (m^2/s).
$\sigma_\varepsilon, \sigma_k$	Turbulent Prandtl number for diffusion of (k) and (ε).
μ_t	Turbulent dynamic viscosity ($N.s/m^2$).
μ	Dynamic viscosity ($N.s/m^2$).
δ_x, δ_y	Inter-nodes distance (m).
λ	Convergence criteria
σ_t	Turbulent Prandtl number.
ρ	Density (kg/m^3).
Γ_{eff}	Effective diffusion coefficient.
ν_x, ν_y	Mean velocity components in x and y direction (m/s).

θ Excess temperature.

1. Introduction

The atmospheric conditions which affect human comfort are temperature, humidity, air purity, and air-movement, however, comfort conditions for human habitation are normally specified in term of temperature and air velocity. In any conditioned space, these parameters depends on number of factors including the dimensions of the room, size of the windows, room turbulence, the outside weather conditions and the location of the heating or cooling systems. It is important to understand the way in which these factors affect the pattern of air-movement generated in such spaces. At the present time the air-conditioning systems can be classified as winter air conditioning systems and summer air conditioning systems. The major problem of winter air conditioning systems is to heat the air and bring the moisture content up to an acceptable level, so to create the proper combination of temperature and air motion in the occupied zone of the indoor space to satisfy the comfort requirements of the occupants. There are many types of heating systems which are used the present time. One of these types which is used for heating a room is natural convection heaters (e.g., radiator, skirting heaters, cabin convectors, and perimeter continuous heaters) in which the emitted heat is actually transferred to the air of the given space by convection.

2. Theory

2.1 Mathematical formulation

The governing equations, which describe the conservation of mass, momentum and energy for two-dimensional turbulent, incompressible steady flow in a Cartesian coordinate system can be written as follow [1,2].

(i) continuity:

$$\frac{\partial \nu_x}{\partial x}+\frac{\partial \nu_y}{\partial y}=0 \qquad (1)$$

(ii) x-direction momentum:

$$\rho\frac{\partial}{\partial x}\left(\nu_x\nu_y\right)+\rho\frac{\partial}{\partial y}\left(\nu_x\nu_y\right)=\frac{\partial}{\partial x}\left[\mu_{eff.}\frac{\partial \nu_x}{\partial x}\right]+\frac{\partial}{\partial y}\left[\mu_{eff.}\frac{\partial \nu_x}{\partial y}\right]+S_{vx} \qquad (2)$$

(iii) y-direction momentum

$$\rho\frac{\partial}{\partial x}\left(\nu_x\nu_y\right)+\rho\frac{\partial}{\partial y}\left(\nu_y\nu_y\right)=\frac{\partial}{\partial x}\left[\mu_{eff.}\frac{\partial \nu_y}{\partial x}\right]+\frac{\partial}{\partial y}\left[\mu_{eff.}\frac{\partial \nu_y}{\partial y}\right]+S_{vy} \qquad (3)$$

(iv) energy

$$\rho\frac{\partial}{\partial x}\left(\nu_x T\right)+\rho\frac{\partial}{\partial y}\left(\nu_y T\right)=\frac{\partial}{\partial x}\left[\Gamma_{eff.}\frac{\partial T}{\partial x}\right]+\frac{\partial}{\partial y}\left[\Gamma_{eff.}\frac{\partial T}{\partial y}\right]+S_T \qquad (4)$$

$$\Gamma_{eff.}=\frac{m}{s_r}+\frac{m_t}{s_t} \qquad (5)$$

The appropriate sources and/ or sinks of the variables concerned are given below:

$$S_{vx} = \frac{\partial}{\partial x}\left(\mu_{eff.}\frac{\partial v_x}{\partial x}\right)+ \frac{\partial}{\partial y}\left(\mu_{eff.}\frac{\partial v_y}{\partial y}\right)-\frac{\partial p}{\partial x} \quad (6)$$

$$S_{vy} = \frac{\partial}{\partial x}\left(\mu_{eff.}\frac{\partial v_x}{\partial y}\right)+ \frac{\partial}{\partial y}\left(\mu_{eff.}\frac{\partial v_y}{\partial y}\right)-\frac{\partial p}{\partial y}+\rho g\left(\frac{T-T_o}{T_o}\right) \quad (7)$$

The main difficulty in solving these equations concerns the determination of unknown correlation representing turbulent viscosity (m_t) which is not a fluid property and varies over the flow domain, depending on the turbulence condition. Therefore, before any solution can be obtained they must be expressed in terms of a known or calculated quantities. These expressions are called turbulent models.

2.2 Turbulence models

A turbulence model is a set of differential equations governing the distributions of a finite number of statistical properties of the turbulence. It can be classified in several ways. The one most often used is that arranged in order of the number of differential equations solved in addition to the mean flow equations [3].

(i) zero-equation models
(ii) one- equation models
(iii) two- equation models
(iv) stress equation models

The two-equation model (k-e) model has been applied to a large number of different flows, and it shows the capability of handling complex recirlculating flows in much less computer time than other models. This type of turbulence model was adopted for present study. The partial differential equation for the kinetic energy of turbulence (k), and it is dissipation rate (e) can be expressed for two - dimensions Cartesian coordinate as follows [4]:

$$\rho\frac{\partial}{\partial x}(v_x k)+\rho\frac{\partial}{\partial y}(v_y k)=\frac{\partial}{\partial x}\left[\left(\frac{\mu}{\sigma_k}+\frac{\mu_t}{\sigma_k}\right)\frac{\partial k}{\partial x}\right]+ \frac{\partial}{\partial y}\left[\left(\frac{\mu}{\sigma_k}+\frac{\mu_t}{\sigma_k}\right)\frac{\partial k}{\partial y}\right]+G_k-\rho\varepsilon \quad (8)$$

$$\rho\frac{\partial}{\partial x}(v_x \varepsilon)+\rho\frac{\partial}{\partial y}(v_y \varepsilon)=\frac{\partial}{\partial x}\left[\left(\frac{\mu}{\sigma_\varepsilon}+\frac{\mu_t}{\sigma_\varepsilon}\right)\frac{\partial \varepsilon}{\partial x}\right]+ \frac{\partial}{\partial y}\left[\left(\frac{\mu}{\sigma_\varepsilon}+\frac{\mu_t}{\sigma_\varepsilon}\right)\frac{\partial \varepsilon}{\partial y}\right]+C_1\frac{\varepsilon}{k}(G_k)-C_2\frac{\rho\varepsilon^2}{k} \quad (9)$$

and, the generation term is defined as follows:

$$G_k = \mu_t\left[2\left[\left(\frac{\partial v_x}{\partial x}\right)^2+\left(\frac{\partial v_y}{\partial y}\right)^2\right]+\left[\frac{\partial v_x}{\partial y}+\frac{\partial v_y}{\partial x}\right]^2\right] \quad (10)$$

The turbulent viscosity is determined from the values of turbulent kinetic energy (k) and its dissipation rate (e) according to [4]:

$$\mu_t = \frac{\rho C_d k^2}{\varepsilon} \quad (11)$$

The above model contains five empirical constants, which are assigned the values given in table (1), recommended by Launder and Spalding [5,6]:

C_1	C_2	C_d	s_t	s_e
1.44	1.92	0.09	1.0	1.3

Table (1) constants of turbulent model

3 Numerical Solution Procedure

3.1 General PDE to be solved

Equation (1), (2), (3), (4), (8), and (9) all have the general form [7,8,9]:

$$\frac{\partial}{\partial x}(r\,v_x\Phi)+\frac{\partial}{\partial y}(r\,v_y\Phi)=\frac{\partial}{\partial x}\left(\Gamma_\Phi\frac{\partial\Phi}{\partial x}\right)+\frac{\partial}{\partial y}\left(\Gamma_\Phi\frac{\partial\Phi}{\partial y}\right)+S_\Phi \qquad (12)$$

In this equation ,(Φ) is the general dependent variable, (Γ_Φ) is the generation diffusion coefficient, and (S_Φ) is the source term. The general differential equation consists of three terms. These will be called the convection term, the diffusion term and the source term for the scale variable (Φ). The expression for diffusion coefficient (Γ_Φ), and source term (S_Φ) corresponding to each particular variable (Φ) are given in table (2):

Equation	Φ	Γ_Φ	S_Φ
Continuity	1	0	0
x-direction momentum	v_x	μ_{eff}	$-\frac{\partial p}{\partial x}+\frac{\partial}{\partial x}\left(\mu_{eff}\frac{\partial v_x}{\partial x}\right)+\frac{\partial}{\partial y}\left(\mu_{eff}\frac{\partial v_y}{\partial x}\right)$
y-direction momentum	v_y	μ_{eff}	$-\frac{\partial p}{\partial x}+\frac{\partial}{\partial x}\left(\mu_{eff}\frac{\partial v_x}{\partial y}\right)+\frac{\partial}{\partial y}\left(\mu_{eff}\frac{\partial v_y}{\partial y}\right)+\rho g\frac{T_o-T}{T_o}$
Temperature	T	$\frac{\mu}{\sigma}+\frac{\mu_t}{\sigma_t}$	————
Turbulence energy	k	$\frac{\mu_{eff}}{\sigma_k}$	$G_K-r\,\varepsilon+G_B$
Dissipation Rate	ε	$\frac{\mu_{eff}}{\sigma_\varepsilon}$	$C_1\frac{\varepsilon}{K}(G_K+G_B)-C_2\frac{\varepsilon^2}{K}$

Table (2) diffusion coefficients and source terms

where (G_B) is the buoyancy source production term which is added to the (k-ε) equations and it is given by [10].

$$G_B = -\beta g \frac{\mu_t}{\sigma_t} \cdot \frac{\partial \theta}{\partial y} \qquad (13)$$

3.2 Grid and Control Volume

The numerical method, aims to calculate the values of the relevant dependent variables at a set of chosen points called the grid points. The algebraic equation for those values, called discretization equations, is derived by integrating the governing differential equation over a sub-domain referred to as control volumes as shown in Fig. (1). It can be seen that the situation of a near-boundary control volume is shaded too. Here, one face of the control volume coincides with the boundary of the calculation domain, and a boundary grid point is placed at the center of the control volume face. This arrangement makes it rather easy to treat different boundary conditions the shaded control volume can easily accept a given value of (Φ) at the boundary or a given flux through the boundary surface. A typical control volume such as a round point (P) is shown shaded and enclosed by the dashed line in Fig.(2). The grid point (P) communicates with the four neighbouring grid points through the four faces of the control volume. These points are denoted by (E, W, N and S), implying the east, west, north, and south directions with respect to the center point (P).

3.3 The Staggered Grid

All scalar dependent variables, including pressures stored at the main grid points just described, while the velocity components are stored at "staggered" locations, since if the velocity components and the pressure are calculated for the same grid points, some physically unrealistic field arises as the solution. Fig.(3) shows a portion of a two-dimensional grid. The locations for which the velocity components are calculated are shown by short arrows. In the staggered grid, the velocity components are computed for the points lying on the control-volume faces. All other variables including pressure are calculated at the grid points shown by dots. A consequence of this arrangement is that the normal velocity components are directly available at the control-volume faces, where they are needed for calculation of mass flow rates. Furthermore, the pressure difference between two grid points can be used to "drive" the velocity component located between them, the staggered location and control volume for the velocity components are shown in Fig.(4) and Fig.(5).

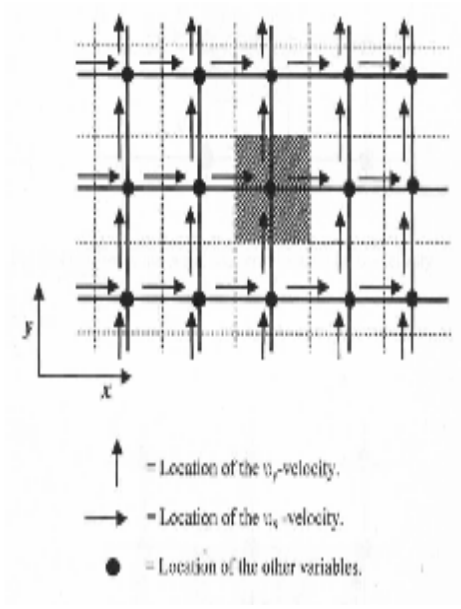

Fig (3) Staggered grid

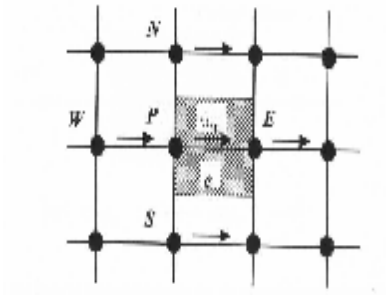

Fig.(4) Control volume and staggered location for v_x -velocity

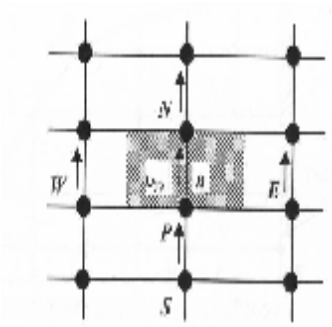

Fig.(5) Control volume and staggered location for v_y -velocity

3.4 General FDE

Equation {12} may be discretized by integration over an element control volume or cell yielding an algebraic equation of the form:

$$a_P \Phi_P = \left(\sum_{E,W,N,S} a\Phi \right) + B \qquad (14)$$

where a_E, a_W, a_N, and a_S are the neighboring coefficient representing the convection and diffusion influence at the four faces of the control volume, in terms of the flow rate {F} and the conductance {D} [11,12]:

$$\left.\begin{aligned} F_e &= (\rho v_x)_e \, \Delta y \\ F_w &= (\rho v_x)_w \, \Delta y \\ F_n &= (\rho v_y)_n \, \Delta x \\ F_s &= (\rho v_y)_s \, \Delta x \end{aligned}\right| \qquad (15)$$

$$\left.\begin{aligned} D_e &= \Gamma_{\Phi,e} \, \Delta y / (\delta x)_e \\ D_w &= \Gamma_{\Phi,w} \, \Delta y / (\delta x)_w \\ D_n &= \Gamma_{\Phi,n} \, \Delta y / (\delta x)_n \\ D_s &= \Gamma_{\Phi,s} \, \Delta y / (\delta x)_s \end{aligned}\right| \qquad (16)$$

3.5 Differencing scheme and solution procedure

The finite-differencing scheme used for solving equation (14) is a hybrid scheme [12]:

$a_E = D_e - F_e/2$ if $-2 \le (Pe)_e \le 2$

$a_E = -F_e$ if $(Pe)_e < -2$

$a_E = 0$ if $(Pe)_e > 2$

where *(Pe)* is a dimensionless quantity called the Peclet number and defined by [13]:

$$Pe = F/D = (\rho v \, \delta / \Gamma_\Phi)$$

The method of solution is referred to as the "SIMPLE algorithm" which is described by Patankar [12] and has been used extensively for solving elliptic flow problems. This method does not employ equations for pressure, instead the pressure in each computational cell is linked to the velocities of the surrounding cells in such a way that conformity with the continuity equation is always observed. This yields a pressure correction equation which gives the pressure change needed to obtained the necessary change in the velocity and / or density so that continuity of flow is satisfied. For this reason it is

necessary to use a staggered grid as shown in Fig.(3), where the quantities (P, T, k, e) are located at point P and the velocity components v_x and v_y are located at the boundaries of the cell. The grid is arranged in such a way that boundaries coincide with control volume walls. At a solid boundary a wall function formulation of Launder and Spalding [4] is used for the points close to the wall. The discretized equation is solved by sweeping the flow field line-by-line at a given x-position starting from bottom to top. The tri- diagonal matrix algorithm (TDMA) is applied for solving the discretized equations. The procedure is repeated for the next line downstream until the whole field is swept.

3.6 Convergence

The convergence criteria for the numerical solution which is applied in the present study is based on the residual of the variable (Φ) at node (P), where the residual from equation (14):

$$R_\Phi = a_p \Phi_p - \left(\sum_{E,W,N,S} a \Phi \right) + B \quad (17)$$

(R_Φ) for an exact solution, must be zero to satisfy the (FDE), but for a nearly exact solution, the normalized residual for the different variable can be defined:

$$\sum_{\text{for all field}} |R_\Phi| \leq \lambda \quad (18)$$

where (l) is a convergence criteria which its adopted value for the present study is less than (1×10^{-5}).

4. The Geometries Considered and Their Boundary Conditions

The geometrical arrangements that have been tested in the present work are illustrated in Fig.(6). The space dimensions are (4 m wide × 3 m high) for both geometries and with a heating source of length (h) and width (b). The values for velocity components, temperature, turbulent kinetic energy and its dissipation rate at the solid boundaries are given in table (3).

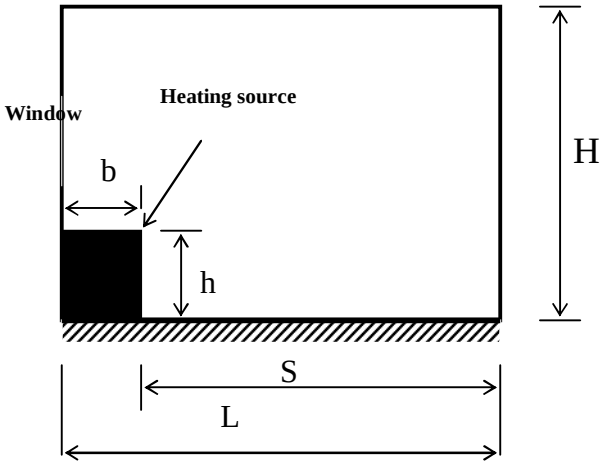

a) Geometry (A).

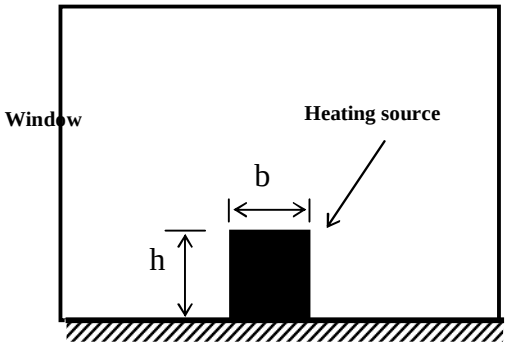

b) Geometry (B).

Fig.(6) Physical domain.

Variable	Boundary conditions at walls			
	Ceiling	Floor	Left-wall	Right-wall
v_x	0	0	0	0
v_y	0	0	0	0
k	The gradients normal to the walls set equal to zero.			
e	0	0	0	0
T (c^o)	15	15	15	15
Temperature of heat source (c^o).				100
Temperature of window (c^o).				10

Table(3) Boundary conditions for geometries A and B.

5. Nusselt number Definitions.

The local Nusselt number is defined as [14]:

$$Nu = \frac{h_{cx}.x}{k_c} \qquad (19)$$

where, (h_{cx}) is the local heat transfer coefficient in turbulent flow over a plane surface [14]:

$$h_{cx} = \frac{k_c \left(\partial T/\partial n\right)\big|_W}{\left(T_W - T_m\right)} \qquad (20)$$

The average Nusselt number is obtained by integrating eq.(19) as [14]:

$$\overline{Nu} = \frac{1}{\left(T_W - T_m\right)} \int_0^L \left(\partial T/\partial n\right)\big|_W \, dx \qquad (21)$$

6. Results and Discussion

The buoyant flow patterns induced by heating source in the rectangular space with isothermal side walls and cold window for geometries (A and B) are presented with temperature isothermal lines in Figs.(7-8) in terms of velocity vectors and temperature contours. The computed flow patterns in geometry (A) for three different sizes of the heating source (b/h =0.08, 0.25 and 0.5) are presented in Fig.(7). This figure illustrates that the heating source creates an upward hot air stream along the left wall which overcome the cold downdraught and then moves horizontally along the ceiling and cools as it flows vertically downward a long the right wall. Furthermore, these patterns show that as the size of the heating source increases the circulation is seen to increase inside the space giving rise to two different recalculating zones and maintaining a good mixing of the air inside the space. Fig.(8) represents the buoyant flow patterns in geometry (B) with size of the heating source as (b/h = 0.75, 1.45, and 6.0). The cold flow falls rapidly towards the floor and then horizontally toward the heating source which causes an upward hot air movement in the adjacent regions. The mixing of these two air-streams leads to the generation of high velocity, which produces a local thermal discomfort in the space. The temperature contours inside the two geometries show that geometry (A) with heating size (b/h=0.5) gave acceptable and comfortable limits of the temperature inside the occupation zone than geometry (B). Figs.(9-10) show the local Nussuelt number for all surfaces of the space in geometries (A and B). It can be seen that as the temperature near the hot surfaces increases the rate of heat transfer increase. This is because the local Nusselt number is affected by the distance and temperature difference near the wall. Also it is clear that the rate of heat transfer along the ceiling and right wall in geometry (A) is not affected by the heating source size. Figs.(11-12) show the variation of average Nusselt number with the size of the heating source for both geometries (A and B). It can be concluded that the

geometry (B) gives a higher rate of heat transfer than geometry (A) due to larger difference in temperature.

7. Conclusion

The location and size of the heating source are of great importance for thermal comfort in air-conditioned spaces. The location of the heating source under a cold window will give the optimal thermal condition in the occupation zone. This is due to the direct offset of the cold window effect by the heating source. However, the size of the heating source will also improve the occupation zone condition since it increases the rate of heat transfer inside the space. Also, it was found from the second geometrical arrangements of the room that the jet resulting from the mixing of the cold downdraught from the window and hot air stream coming from the heating source create, local thermal discomfort and cannot maintain the desired air temperature in the space.

7. Refrences

1. Kakac S., Aung W. and Viskanta R., " Natural Convection Fundamentals and Applications", chapt. 5, publ. By Hemisphere puble. Corp. Washington, 1985
2. Jaluria Y., "Natural convection heat and mass transfer ", chap.5, Pergamon press, Oxford 1980.
3. Nallasamy M. "Turbulence Models and Their Applications to the Predictions of Internal Flow", Computer and Fluids, Vol. 15, No.2, 1987, PP. (151-195).
4. Launder B.E and Spalding D.B " mathematical models of turbulence", academic press., londoin 1972
5. Launder B.E and Spalding D.B ".The Numerical Computation of Turbulent Flows" comp. Methods appl. Mech. and eng., vol.3, 1974, PP.269-289.
6. Ostrach S., "Natural convection in Enobsurces" , Jornal of heat transfer, Vol. 110, 1988, PP. 1175-1189.
7. Awbi H. B. and Strak A. A., "Numerical solution of ventilation air jet", the fifth int. Symposium on The Use of Computer For Environmental
8. Haghighat F., jaing Z.and Wang J. C.Y., "Natural convection and air flow pattern in a partitioned room with turbulent flow, ASHRAE, vol.95, part, 1989.
9. Patankar, S. V. "A Calculation Procedure for Two-Dimensional Elliptic Situation", Numerical Heat Transfer, Vol.4, PP 541- 550, 1981.
10. Markots N. C., Malin M.R. and Cox G., "Mathmetical Modeling of Buoyancy- Include Smoke Flow In Enclosures"; Int. J Heat Mass Transfer, Vol. 25, No.1 , 1982, pp. 63-74
11. Mohammad W. S., "Space Air Conditioning of Mechanically Ventilated Room: Computation of Flow and Heat Transfer", Ph.D Thesis , Cranfield Institute of Technology, 1986, UK.
12. Patankar S. V. "Numerical Heat Transfer and Fluid Flow" McGraw Hill, New York,1980.
13. Jatatilleke C. L. V., "The Influence of Prandtle Number and Surface Roughness on The Resistance of The Laminar-Sub-Layer To Momentum and Heat Transfer". Progress In Heat and Mass Transfer. Vol., 1968, pp. 193-329.
14. Frank Kreith and Mark S. Bohn, "Principle of Heat Transfer", Fifth Edition, Copyright 1997.

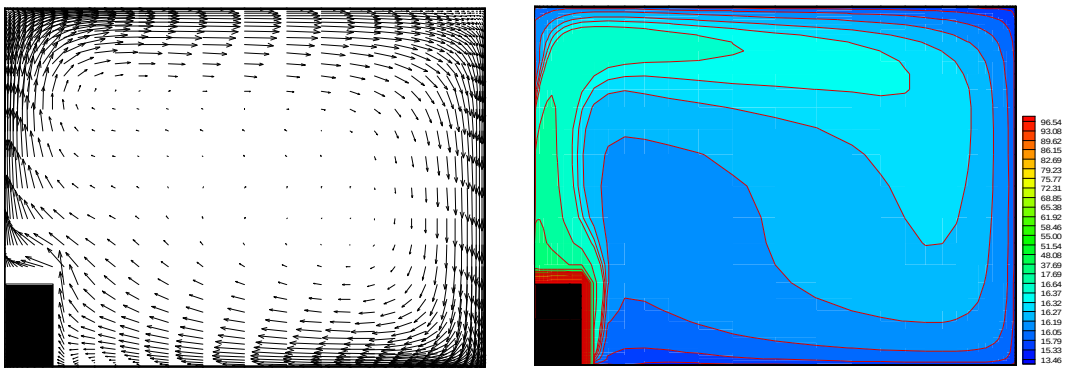

a) For b/h=0.08

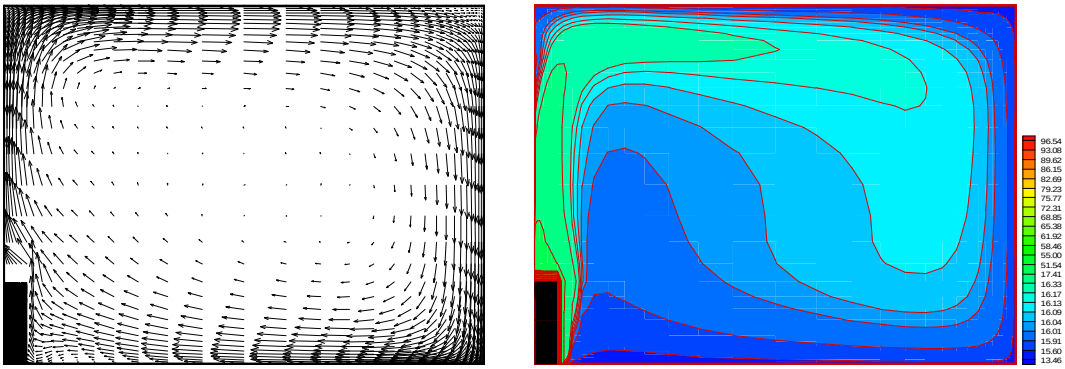

b) For b/h=0.28

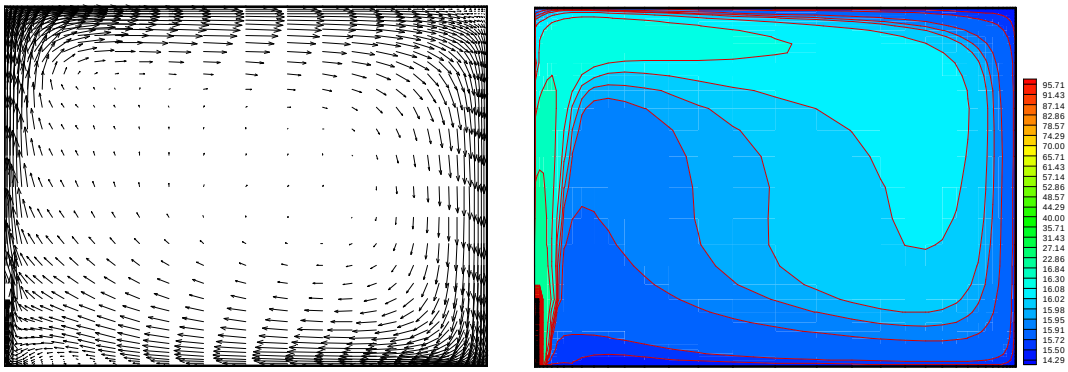

c) For b/h=0.5

Fig.(7) Flow patterns and isothermal lines for geometry (A). Temperature range (13.46-96.54 c^{o}

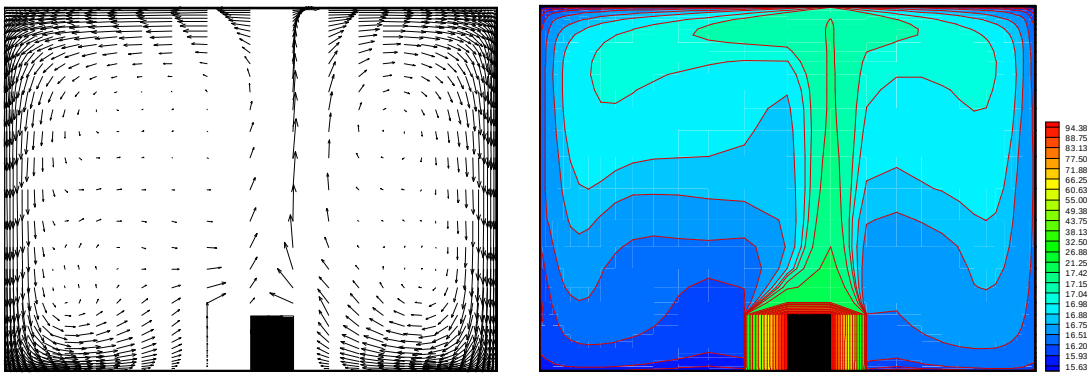

a) For b/h=0.75

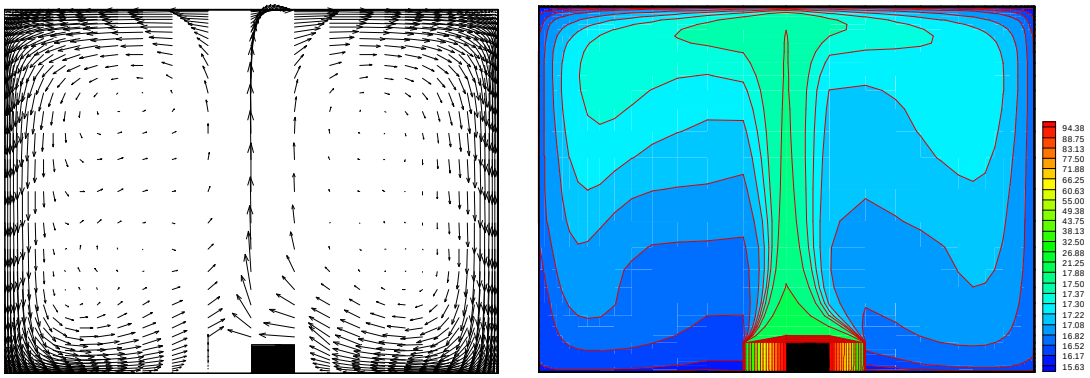

b) For b/h=1.45

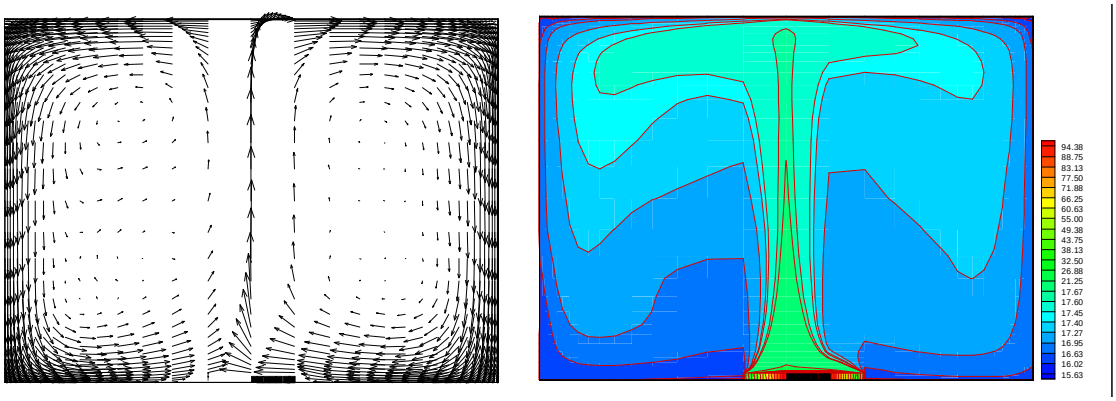

c) For b/h=6

Fig.(8) Flow patterns and isothermal lines for geometry (B). Temperature range (15.63-94.38 c^{o})

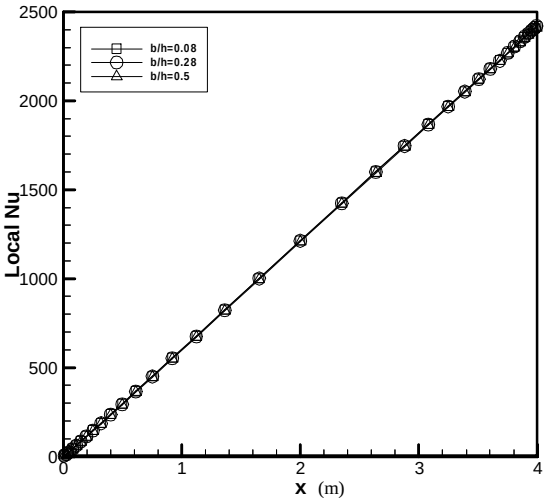

Ceilin

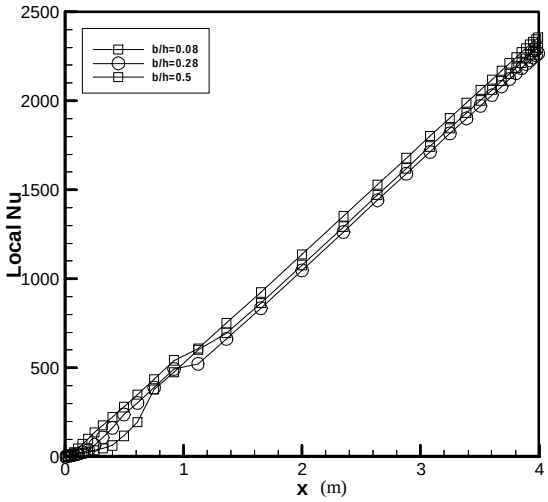

Floor.

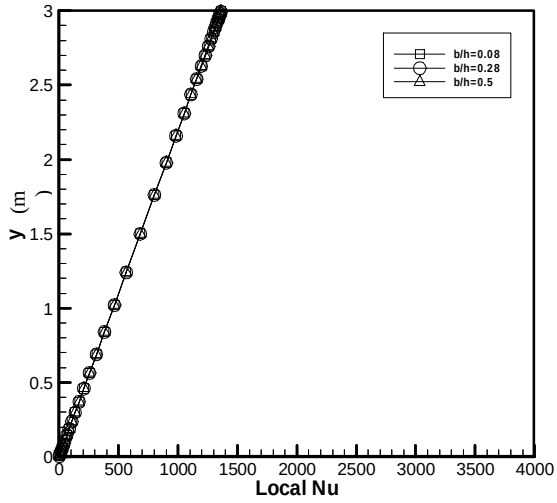

Right

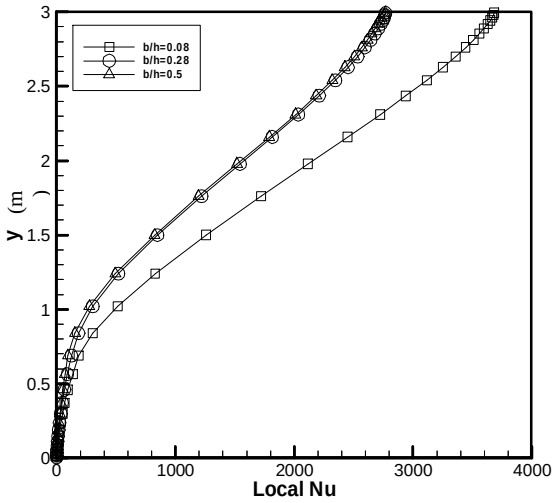

Left wall

Fig.(9) Local Nusselt number for geometry (A).

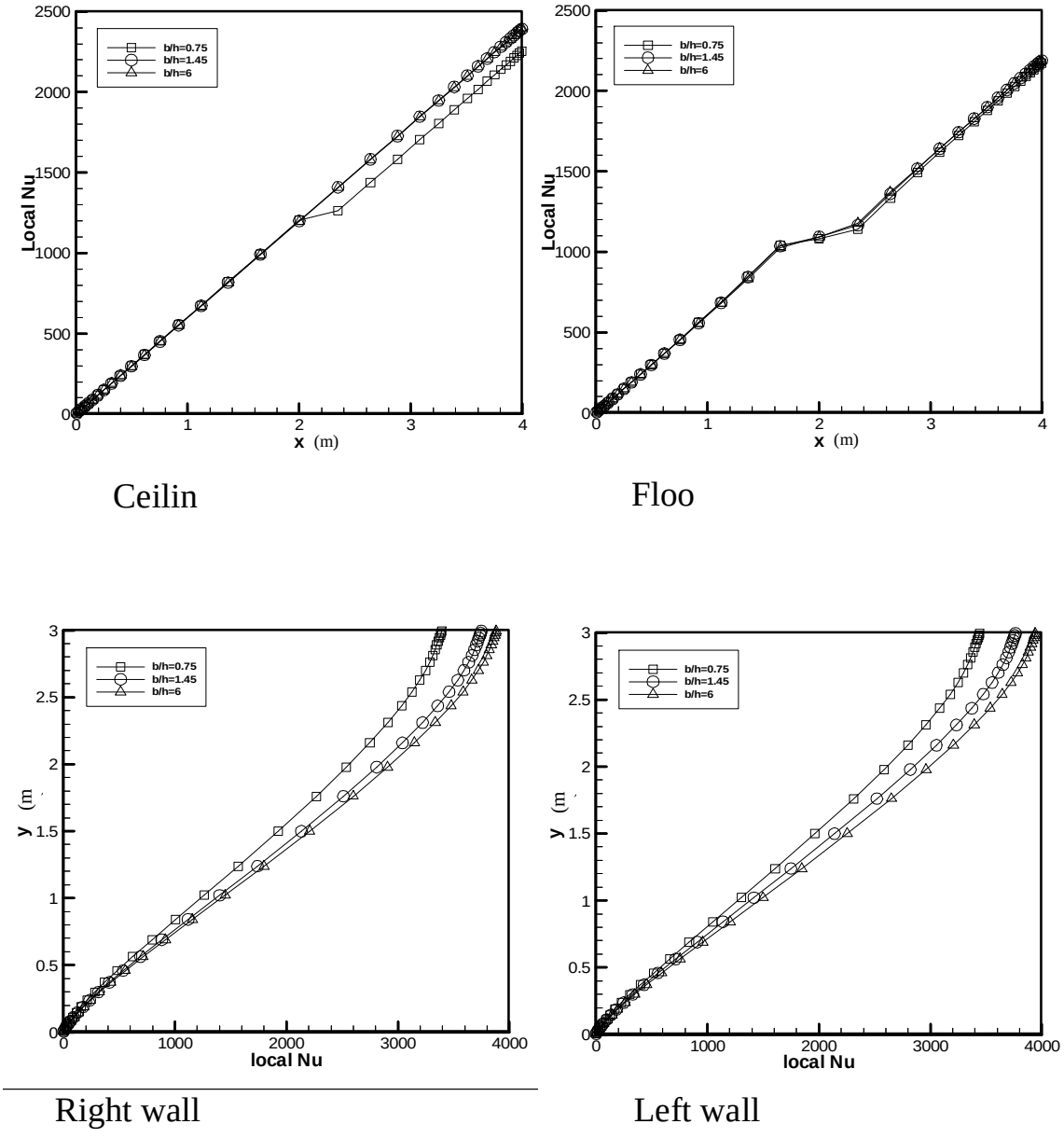

Fig.(10) Local Nusselt number for geometry (B).

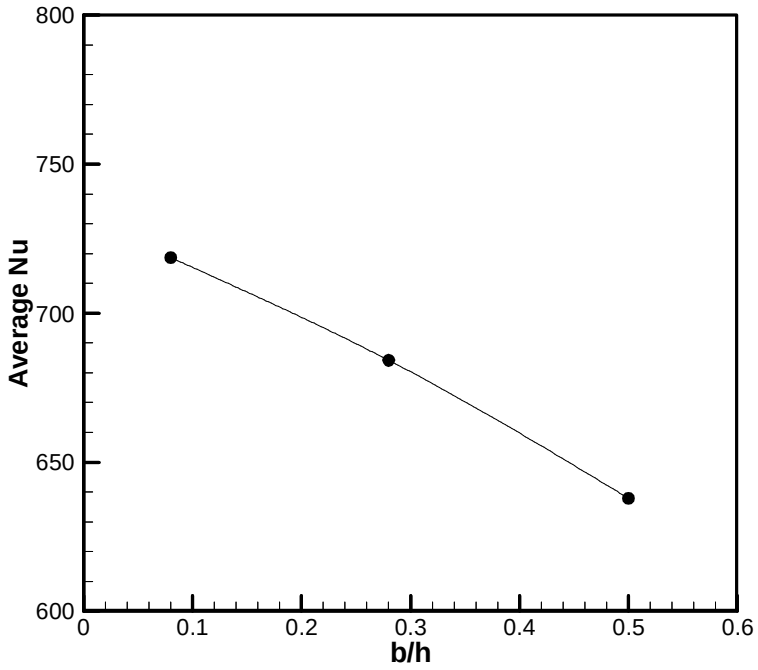

Fig.(11) Average Nusselt number for geometry (A).

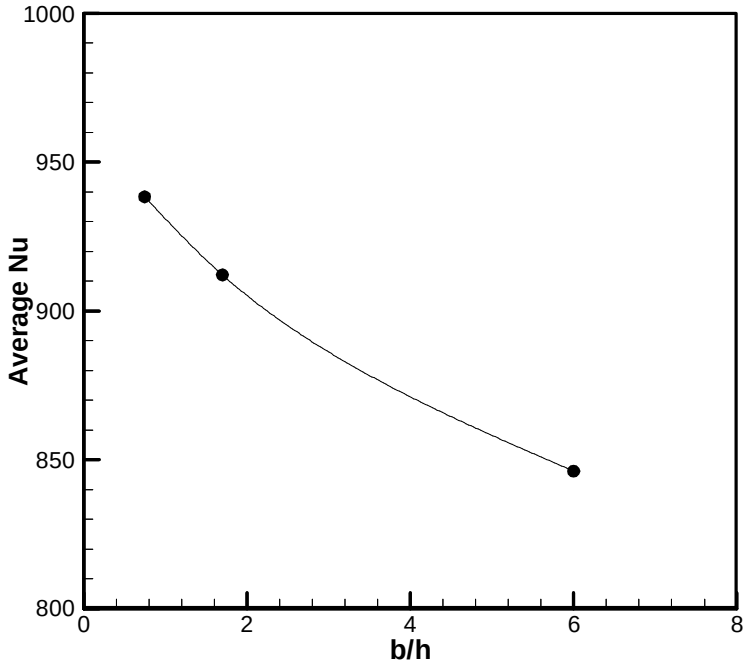

Fig.(12) Average Nusselt number for geometry (B).